Supplementary Material

Data availability

Our microCT data can be publicly viewed online through Neuroglancer: (http://neuroglancer-demo.appspot.com/) with http://nova.kasthurilab.com:8000/neuroglancer/recon_crop8_neurog/image as the precomputed source link. Raw data will be made available from the corresponding author upon reasonable request.

dMRI diffusion gradient directions

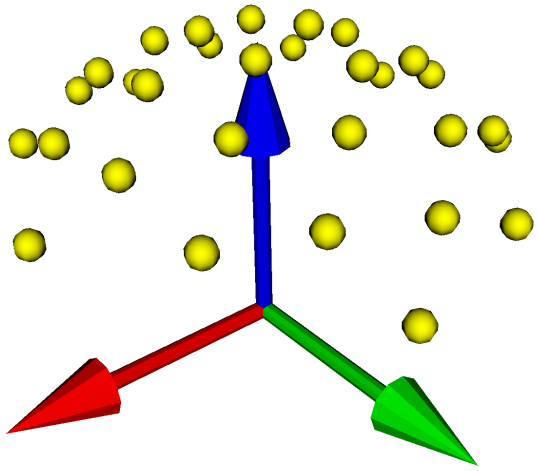

Supporting Information Figure S1. Yellow points represent the direction of each of the 30 noncolinear diffusion gradients used for the dMRI data. Axis orientations are encoded with color, with red encoding left–right, green anterior–posterior, and blue encoding the superior–inferior direction. As can be seen here, a software error led to nonuniform sampling of the diffusion gradients, with oversampling along the super–inferior axis and undersampling of the orthogonal plane. For this reason, we chose to forego quantitative evaluation of dMRI performance and instead present qualitative demonstrations of the utility of microCT.

dMRI–microCT registration results

Supporting Information Video S1 presents a visualization of spatial registration results between microCT and dMRI fODFs. Axial slices of fODFs and intensity data covering the whole brain are shown side-by-side, with microCT on the left and dMRI on the right.

Structure-tensor analysis

For each voxel, the structure tensor is constructed by taking the outer product of the image intensity gradient vector with itself, followed by averaging over a local neighborhood. The result is a symmetric, 3×3, semi-positive definite tensor at each voxel. The eigenvector of the tensor corresponding to the smallest eigenvalue indicates the direction of smallest intensity variation in the local neighborhood. For voxels representing nerve fibers, we make the assumption that this eigenvector is parallel to the local fiber orientation. Confidence in the orientation estimate can be represented by a scalar fractional anisotropy metric constructed from the eigenvalues of the tensor:

$$\text{FA} = \sqrt{\frac{1}{2}\frac{(\lambda_1-\lambda_2)^2+(\lambda_1-\lambda_3)^2+(\lambda_2-\lambda_3)^2}{\lambda_1^2+\lambda_2^2+\lambda_3^2}}, \tag{1}$$

where λ_1, λ_2, and λ_3 represent the first, second, and third eigenvalues of the structure tensor at each voxel. This metric is bounded from 0 to 1, where a higher value represents more confidence in the orientation estimate.

fODF generation

The voxel-wise orientation estimates were used to directly construct fODFs within larger regions of interest (ROIs) across the whole brain. First, the data were divided into cubic ROIs the same size as the corresponding dMRI voxels (150 μm). Of the $N \approx 2\times10^6$ total microCT voxels in each dMRI-voxel-sized region, N' voxels containing fibers were identified by thresholding the raw grayscale values to discard voxels representing microvasculature (GV $\geq$ 38), as well as by thresholding the FA metric to discard voxels with low orientation confidence (FA $\geq$ 0.7). Within each region, the fODF, ψ, can be directly expressed as the sum of N' fiber orientations represented as Dirac delta functions in spherical coordinates (2, 3),

$$\psi(\theta,\phi) = \frac{1}{N}\sum_{j=1}^{N'}\delta(\cos\theta-\cos\theta_j)\delta(\phi-\phi_j), \tag{2}$$

where $\theta \in [0,\pi]$ and $\phi \in [0,2\pi]$ are the polar and azimuth angles, respectively, and j indexes the N' fiber orientations.

ψ represents a band-unlimited distribution of voxel-wise fiber orientations in a specified region of microCT data. It is convenient to expand ψ onto a finite (i.e., band-limited) number of spherical harmonic functions for computational ease and direct comparison with dMRI-derived fODF representations. It can be shown (4) that the spherical harmonic coefficients, Ψ_ℓ^m, of a sum of N' discrete orientations are given by

$$\Psi_\ell^m = \frac{1}{N}\sum_{j=1}^{N'}\bar{Y}_\ell^m(\theta_j,\phi_j), \tag{3}$$

where Y_ℓ^m is the spherical harmonic function of degree ℓ and order m and the overbar denotes a complex conjugate. As with dMRI, we assume that these fODFs have even symmetry, so coefficients were calculated for even harmonic degrees. For this study, we chose to expand the fODF to $\ell_{\text{max}} = 8$, in accordance with recommendations for the highest ℓ_{max} typically used in dMRI studies (1).

Fiber density

Because each fODF was generated from N' separate orientation estimates but normalized by $N \approx 2 \times 10^6$, where $N' < N$ (Eq. 3), the relative size of the fODFs reflects the fraction of microCT voxels within each ROI that were identified as containing valid fibers. The fraction of identified fiber voxels can be calculated directly from the c_{00} coefficient of the SH representation of the fODFs:

$$\text{FD} = \frac{N'}{N} = \frac{c_{00}}{Y_0^0}, \tag{4}$$

where FD is a proxy for the fiber density within each ROI and $Y_0^0 = \sqrt{1/4\pi}$ is the constant $\ell = 0$ SH function.

References

1. Tournier JD, Calamante F, Connelly A. Determination of the appropriate b value and number of gradient directions for high-angular-resolution diffusion-weighted imaging. *NMR in Biomedicine.* 2013;26:1775–1786.

2. Alimi A, Ussou Y, Pierre-Simon J, Michalowicz G, Deriche R. An Analytical Fiber ODF Reconstruction in 3D Polarized Light Imaging. in *15th IEEE International Symposium on Biomedical Imaging (ISBI)*(Washington, D.C.):1276–1279 2018.

3. Deslauriers-Gauthier S, Marziliano P, Paquette M, Descoteaux M. The application of a new sampling theorem for non-bandlimited signals on the sphere: Improving the recovery of crossing fibers for low b-value acquisitions. *Medical Image Analysis.* 2016;30:46–59.

4. Deslauriers-Gauthier S, Marziliano P. Sampling Signals With a Finite Rate of Innovation on the Sphere. *IEEE Transactions on Signal Processing.* 2013;61:4552–4561.